metals

MDPI

Review

Advances in Superplasticity from a Laboratory Curiosity to the Development of a Superplastic Forming Industry

Jittraporn Wongsa-Ngam [1] and Terence G. Langdon [2,*]

[1] Department of Mechanical Engineering, School of Engineering, King Mongkut's Institute of Technology Ladkrabang, Bangkok 10520, Thailand
[2] Materials Research Group, Department of Mechanical Engineering, University of Southampton, Southampton SO17 1BJ, UK
* Correspondence: langdon@soton.ac.uk

Abstract: Superplasticity refers to the ability of some materials to pull out to tensile elongations of 400% or more when the strain rate sensitivity is ~0.5. The first report of true superplastic flow was published in 1934 in experiments conducted in England. However, this remarkable result attracted little interest among western scientific researchers and the result remained a laboratory curiosity for many years. Later, following extensive research on superplasticity in the Soviet Union, interest developed in the west, and superplasticity became a topic of extensive scientific research. This research was further enhanced with the demonstration that the application of severe plastic deformation provided an opportunity for achieving grain refinement to the submicrometer or even the nanometer level, and these small grains were especially attractive for achieving good superplastic properties. It is now recognized that superplastic alloys provide an excellent forming capability, especially in making high quality curved parts that are not easily fabricated using more conventional processes. This has led to the development of a large superplastic forming industry that currently processes many thousands of tons of sheet metals. This report traces these developments with an emphasis on the scientific principles behind the occurrence of superplastic flow.

Keywords: flow mechanism; grain boundary sliding; severe plastic deformation; strain rate sensitivity; superplastic forming

Citation: Wongsa-Ngam, J.; Langdon, T.G. Advances in Superplasticity from a Laboratory Curiosity to the Development of a Superplastic Forming Industry. *Metals* **2022**, *12*, 1921. https://doi.org/10.3390/met12111921

Academic Editors: Marcello Cabibbo and Sergiy V. Divinskiy and Ayrat Nazarov

Received: 30 September 2022
Accepted: 7 November 2022
Published: 9 November 2022

1. Introduction

When metals and other crystalline materials are subjected to the application of a constant load, they typically exhibit the following three distinct regions of flow: there is an initial primary region in which the flow rate decreases with increasing strain, then a secondary or steady-state region in which the flow rate remains reasonably constant and finally there is a tertiary stage where the rate of flow increases to final failure. In practical applications, the secondary or steady-state region is important because it generally accounts for a large fraction of the total strain. The creep rate in this steady-state region, $\dot{\varepsilon}$, may be expressed through a general relationship of the form [1–3].

$$\dot{\varepsilon} = \frac{ADG\mathbf{b}}{kT}\left(\frac{\mathbf{b}}{d}\right)^{p}\left(\frac{\sigma}{G}\right)^{n} \quad (1)$$

where D is the appropriate diffusion coefficient defining the creep flow mechanism (equal to $D_o \exp(-Q/RT)$ where D_o is a frequency factor, Q is the activation energy for the diffusive process, R is the gas constant and T is the absolute temperature), G is the shear modulus, $\mathbf{b}$ is the Burgers vector, k is Boltzmann's constant, d is the grain size, σ is the applied stress, p and n are the exponents of the inverse grain size and the stress, respectively, and A is a dimensionless constant. The stress exponent, n, is equivalent to $1/m$, where m is defined as

the strain rate sensitivity, which is used when materials are pulled into a testing machine at a constant rate.

Usually, when metals are deformed, even at elevated temperatures, they tend to break at relatively low total elongations that are typically less than 100%. However, early experiments showed that it was also possible to test some materials and achieve exceptionally high elongations prior to failure. For example, in 1912, an elongation of 163% was achieved in brass [4], and in 1928, there was a report of an elongation of ~300% in Cd-Zn and Pb-Sn alloys [5]. Finally, in 1934, Pearson in England achieved the remarkable results of tensile elongations of ~1950% in a near-eutectic Bi–Sn alloy and ~1505% in a Pb-Sn alloy [6]. These elongations were easily the largest reported up to that time, and the sample of the Bi–Sn alloy is shown in Figure 1, where it is coiled for convenient photography.

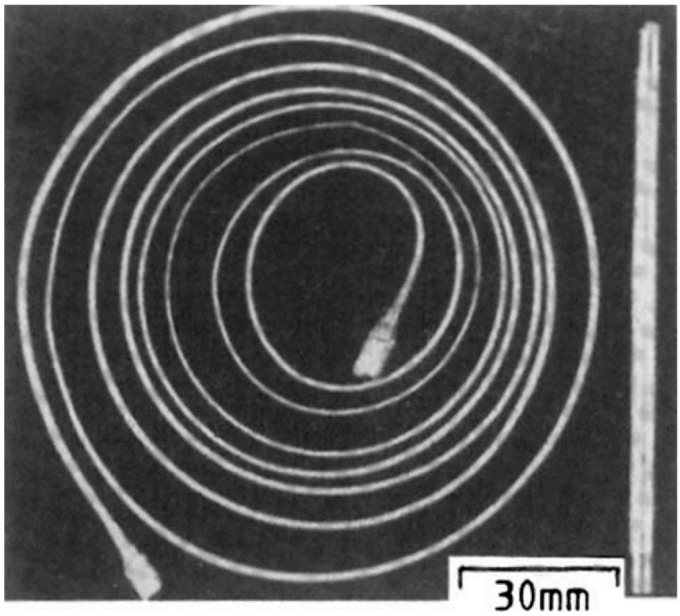

Figure 1. Tensile elongation of ~1950% achieved in a Bi–Sn alloy [6].

To place these results in context, it is first necessary to examine the flow behavior of metals at elevated temperatures. An important result in 1969 was the demonstration that, by analyzing a large number of published results, the tensile elongations attained for all metals increased directly with increasing values of the strain rate sensitivity, m [7]. This result is shown in Figure 2, where the measured values of m are plotted against $\Delta L/L_o$%, where ΔL is the total increase in length at the point of fracture, and L_o is the initial gauge length as follows: Figure 2 includes both the original data and two sets of results obtained later showing exceptional elongations in the Zn-22% Al eutectoid alloy [8] and the Pb-62% Sn eutectic alloy [9]. It is readily apparent from Figure 2 that all datum points scatter about a single line, with high elongations requiring a high value of m and therefore a low value of the stress exponent, n.

In practice, the value of n for any specific experimental testing condition is governed by the flow process controlling the rate of deformation during testing. Several mechanisms have been developed for flow in high temperature creep, and these are described in detail in earlier reports [1,2]. If flow occurs through the stress-directed diffusion of vacancies without any dislocation activity, the process is known as diffusion creep where $n = 1$. There are two types of diffusion creep since the vacancies may flow either through the crystalline lattice in Nabarro-Herring creep [10,11] where $p = 2$ and $Q = Q_\ell$ in Equation (1) where Q_ℓ is the activation energy for self-diffusion or along the grain boundaries in Coble creep [12] where $p = 3$ and $Q = Q_{gb}$ where Q_{gb} is the activation energy for grain boundary diffusion.

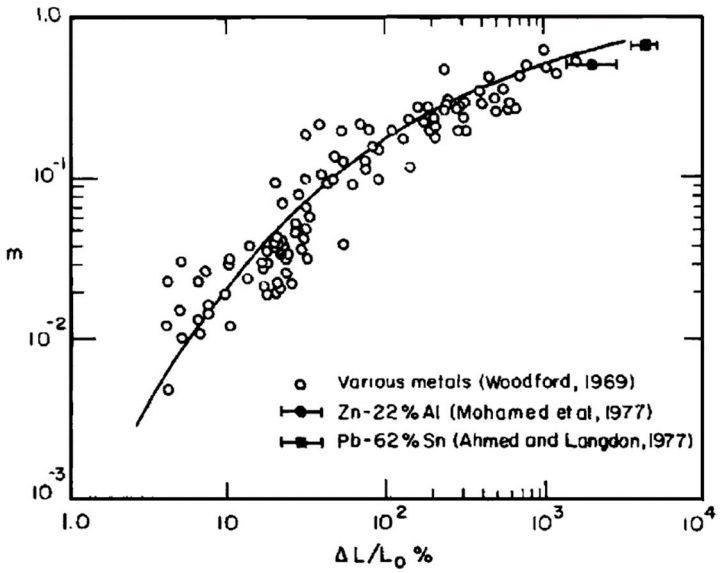

Figure 2. Strain rate sensitivity versus elongation to failure for various metals [7] including results for Zn–22% Al alloy [8] and Pb–62% Sn alloy [9].

If flow occurs through the movement of dislocations, it is generally assumed that dislocation loops expand outwards on different slip planes from Frank–Read sources and the leading edge dislocations become blocked by interactions between the stress fields of dislocations on different but parallel slip planes so that these leading dislocations climb together and annihilate [13]. For creep controlled by the rate of dislocation climb, it was shown that $n \approx 4.5$, $Q = Q_\ell$ and $p = 0$ [14], where the precise value of the stress exponent is dependent upon the value of the stacking fault energy [15]. Although this behavior applies to pure metals, there may be a preferential segregation of solute atoms around the moving dislocations in the form of impurities or Cottrell atmospheres [16], and this may lead to a situation where the rate of glide of the dislocations is slower than the rate of climb so that glide governs the creep behavior. For these conditions, termed viscous glide, the flow rate is again given by Equation (1), but with $n = 3$, $Q = Q_i$ where Q_i is the activation energy for interdiffusion of the solute and again $p = 0$ [17].

The preceding analysis provided a comprehensive summary of flow processes in conventional materials, but it is now necessary to examine the flow processes associated specifically with materials exhibiting exceptionally high elongations. The objective of this report, therefore, is to examine the flow process associated with superplasticity in conventional laboratory testing, to demonstrate the extension and the implications of this approach when using materials with exceptionally small grain sizes and finally to show that there is a considerable potential for using superplasticity in industrial forming applications. These analyses are presented in the following sections.

2. The Flow Process in Superplasticity

Surprisingly, the remarkable result by Pearson in England in 1934 [6], with a tensile elongation of ~1950% in a Bi–Sn alloy, received little or no serious attention in western scientific circles and the result simply became relegated as a laboratory curiosity. However, the work attracted attention in the Soviet Union, where extensive research was undertaken to evaluate the potential for achieving these very high elongations in other materials. The subsequent abstracting of this Russian work in English led to the introduction of the word "superplasticity" in Chemical Abstracts in 1947 [18], where this was a direct translation of the Russian *sverkhplastichnos*' meaning "ultrahigh plasticity". A detailed review of the Russian work published in 1962 [19] prompted an interest in the superplastic effect among western researchers, and this led to the initiation of superplastic experiments at MIT [20] and later at many other universities and institutes around the world.

These early experiments on superplastic flow demonstrated that superplastic elongations require a reasonably high testing temperature, typically above ~0.5 T_m where T_m is the absolute melting temperature of the material, and they also require the use of materials having very small grain sizes, typically smaller than ~10 μm. A comprehensive review of the mechanical characteristics of superplastic materials was presented earlier [21]. Nevertheless, there was no clear understanding of the precise relationship between the applied strain rate in tensile testing and the measured flow stress. The major reason for this problem was that experiments were typically conducted where a single sample was pulled at a fixed strain rate to measure the flow stress and then, using the same sample, additional flow stresses were measured at other strain rates. By conducting the experiments in this way, the results were obtained fairly quickly because of the use of only one sample, but there were major inconsistencies between different sets of results due, in part, to the occurrence of grain growth during the testing procedure.

To avoid this problem, experiments were conducted on a Zn-22% Al eutectoid alloy in which each tensile test was conducted to failure using a different strain rate but the same testing temperature. The result is shown in Figure 3, where the tests were conducted at 473 K using specimens with an initial grain size of 2.5 μm. The lower plot shows the variation of the flow stress with the imposed strain rate and the upper plot shows the separate elongations to failure where each point represents a different sample [22]. These results demonstrate conclusively that there are three separate regions of flow, designated regions I, II and III, where superplasticity occurs in region II and there are reductions in the measured elongations at both slower and faster strain rates in regions I and III, respectively. Measurements showed the strain rate sensitivities were ~0.5 in region II, with reductions to ~0.2 in regions I and III.

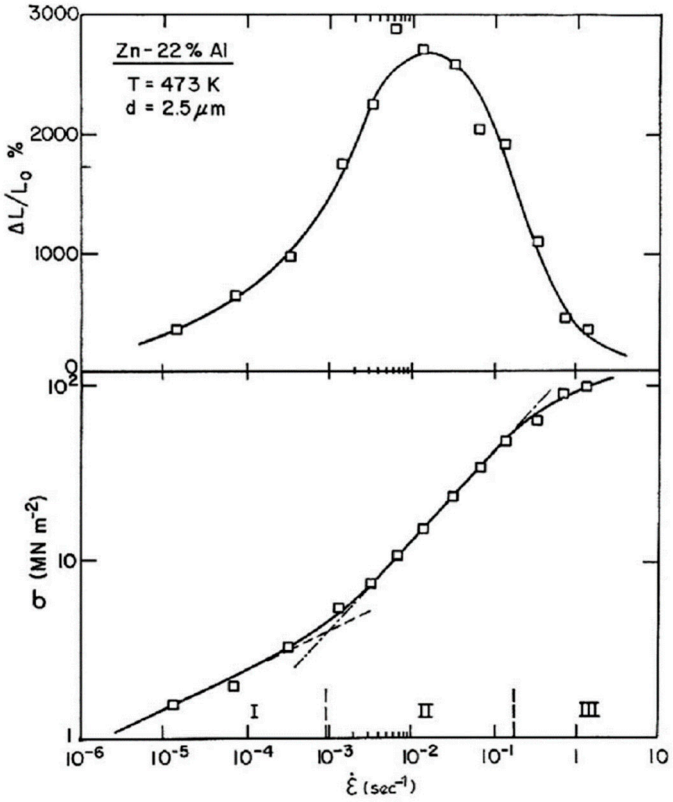

Figure 3. Elongation to failure (upper) and flow stress (lower) plotted against the imposed strain rate for samples of Zn–22% Al alloy tested in tension at 473 K [22].

When a material pulls out to a very high elongation, inspection shows that the material flows without the opening of any significant internal cavitation and, in addition, the grains

remain reasonably equiaxed so that they move over each other during the flow process and the fundamental mechanism of superplasticity is grain boundary sliding, GBS [23]. Nevertheless, GBS cannot occur in isolation and there must be some accommodating mechanism to prevent the opening of voids within the material. In practice, careful experiments showed that the GBS is accommodated by intragranular slip within the grains, but this slip is oscillatory in nature and makes no significant contribution to the overall straining of the polycrystal [24].

In order to achieve a better understanding of the significance of the different regions of flow shown in Figure 3, a deformation mechanism map was constructed where the normalized grain size, $d/\mathbf{b}$, was plotted against the normalized shear stress, τ/G, as shown in Figure 4, where τ is the shear stress, which is plotted directly on the upper axis of the map [25]. This plot shows the regions of Nabarro–Herring and Coble creep at the lower stresses as derived from the theoretical models and then the experimental regions I, II and II at higher stresses. When the flow process is controlled by dislocation climb, it is well established that subgrains are formed during the primary stage of creep and these subgrains have an average size, λ, which varies inversely with the applied stress and remains constant in the region of steady-state flow. Detailed experiments showed that the subgrain size in all metals follows a relationship of the form $\lambda/\mathbf{b} \approx \delta(\tau/G)^{-1}$ where δ is a constant having a value of ~10 [15]: a similar relationship also applies to the flow of ceramic materials [26]. Putting $d = \lambda$ so that the grain size is equal to the subgrain size, it is apparent from Figure 4 that the broken line representing this condition corresponds essentially exactly with the experimental boundary separating regions II and III on the deformation mechanism map. This demonstrates that superplasticity requires a grain size that is smaller than the average subgrain size, and it shows that superplasticity occurs when the intragranular dislocations accommodating GBS are able to move through the grains without encountering any subgrain boundaries that would effectively act as barriers to their movement.

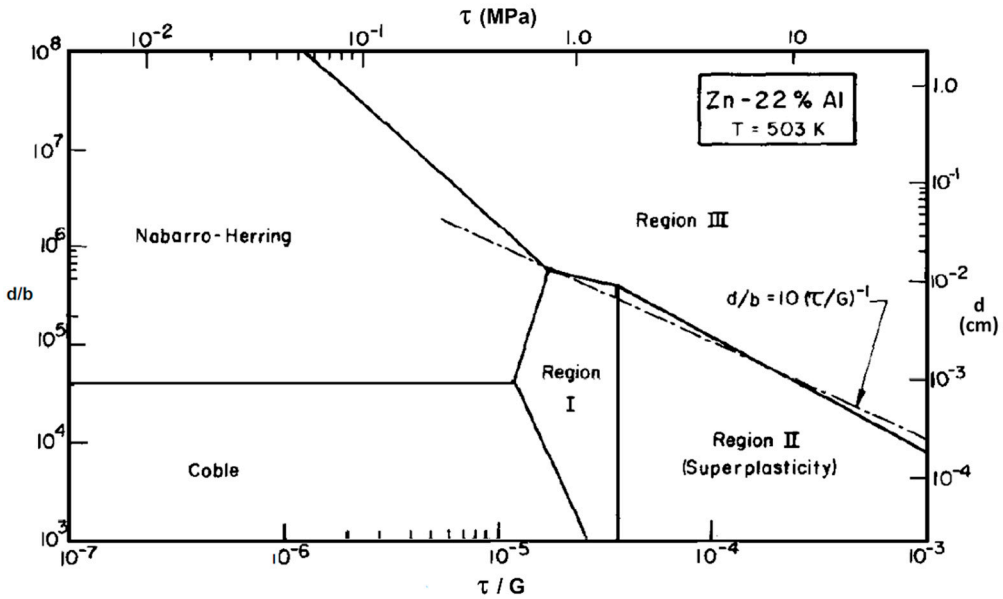

Figure 4. Deformation mechanism map for Zn–22% Al at a temperature of 503 K [25].

Using this approach, it is then possible to illustrate the nature of superplastic flow as shown in Figure 5, where (a) represents conventional creep for materials with large grain sizes so that $d > \lambda$ and (b) shows superplastic flow where $d < \lambda$ [27]. This illustration provides a unified depiction of the nature of grain boundary sliding for materials having different grain sizes. In conventional creep, GBS occurs by the movement of dislocations along the grain boundary and this leads to a stress concentration at the triple point A in

Figure 5a, which is accommodated by an intragranular slip in the next grain where this slip impinges on the subgrain boundary at B. Conversely, in superplastic flow, there is a stress concentration at C, which produces accommodating slip in the next grain and the dislocations are now able to move across the grain without hindrance and impinge on the opposite grain boundary at D. A unified model for these two situations leads to $n = 3$, $p = 1$, $D = D_\ell$ and $A \approx 10^3$ for conventional creep in Figure 5a, where D_ℓ is the coefficient for lattice self-diffusion and $n = 2$, $p = 2$, $D = D_{gb}$ and $A \approx 10$ for superplasticity in Figure 5b, where D_{gb} is the coefficient for grain boundary diffusion [27]. The values predicted for the various parameters in superplasticity are generally in good agreement with experimental data, as shown, for example, by the results in Figure 3.

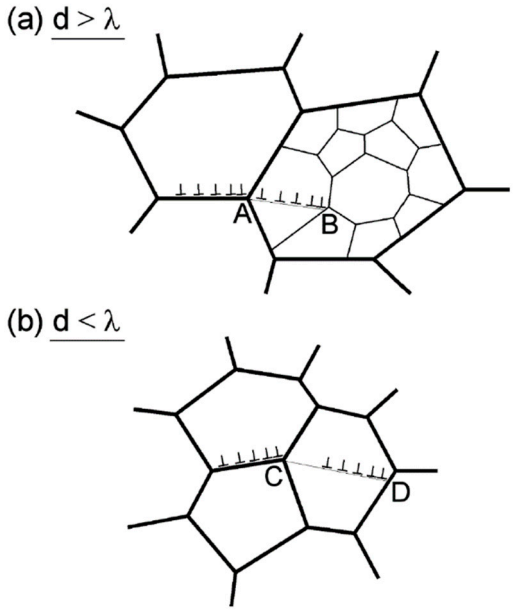

Figure 5. The mechanism of grain boundary sliding (**a**) in conventional creep when $d > \lambda$ and (**b**) in superplasticity when $d < \lambda$ [27].

Finally, it is important to note from Figure 1 that larger elongations are achieved for higher values of m and control by viscous glide has $n = 3$, so that $m \approx 0.3$ whereas superplastic flow has $n = 2$ so that $m \approx 0.5$. This demonstrates that reasonably high elongations may be achieved when viscous glide is the rate-controlling process, and an examination of published results shows there are reports for coarse-grained Al–Mg alloys of elongations up to and slightly exceeding 300% when viscous glide is the controlling process [28]. Based on this analysis, superplasticity may be defined formally as an elongation to failure of at least 400% and a strain rate sensitivity close to ~0.5 [29].

3. The Extension of Superplastic Flow to Submicrometer Grain Sizes

The small grain sizes required for superplastic flow are traditionally achieved by using thermo-mechanical processing, but the smallest grain sizes attained using this procedure are typically in the lower micrometer range of the order to ~3–5 μm. Over the last three decades, alternative procedures have become available that are capable of achieving greater grain refinement and producing materials with submicrometer or even nanometer grain sizes. These procedures are based on the application of severe plastic deformation (SPD), in which a material is subjected to a very high strain but without incurring any significant changes in the overall dimensions of the workpiece. The first example using this approach to achieve superplastic elongations was published in 1988 for an Al-4% Cu-0.5% Zr alloy with a grain size of only 0.3 μm [30], and this early research established the potential for using SPD processing to obtain very small grain sizes [31].

The most important SPD processing technique developed to date is equal-channel angular pressing (ECAP), where a rod or bar is pressed through a die constrained within a channel that is bent through a sharp angle within the die [32]. An example of the results obtained using this technique is shown in Figure 6, where an Al-3% Mg-0.2% Sc alloy was processed by ECAP at different temperatures from 573 to 723 K and the elongations to failure were plotted against the imposed strain rate over more than four orders of magnitude [33]. All of the experimental points relate to different samples, and the results show a general consistency with the earlier results in Figure 3 with very high elongations up to >2000% at intermediate strain rates but with lower elongations at both slower and faster strain rates. These results also demonstrate the occurrence of high strain rate superplasticity, which is defined as the occurrence of superplastic elongations at strain rates at and above 10^{-2} s^{-1} [34]. Moreover, shown in Figure 6 are results obtained by cold rolling (CR) at 673 K, where it is readily apparent that conventional CR cannot achieve the exceptional superplastic elongations that are achieved when processing by ECAP. The elongations of ~200% obtained by CR are typical of the elongations in Al–Mg alloys when deformation occurs by a viscous glide process and the strain rate sensitivity is $m \approx 0.3$.

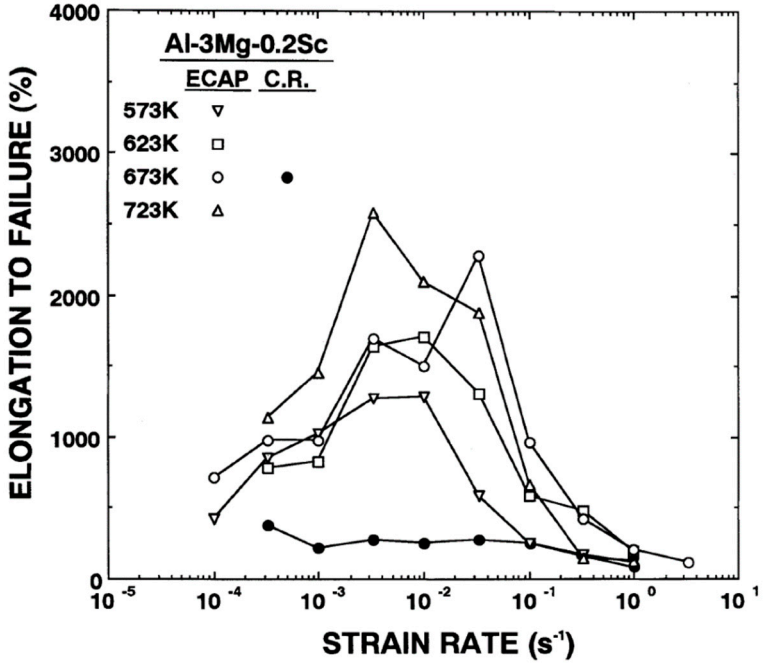

Figure 6. Elongation to failure versus strain rate for an Al–3Mg l–0.2Sc alloy tested after processing by ECAP or cold rolling (CR) [33].

4. The Potential for Achieving Superplasticity at Rapid Strain Rates

By using SPD processing to achieve exceptional grain refinement, it is possible to attain excellent superplastic properties and also reach these very high elongations at rapid strain rates. An example is shown in Figure 6, and it is important to now examine the characteristics of this behavior. The schematic illustration in Figure 7 shows the elongation to failure as a function of the imposed strain rate on a logarithmic scale for two different grain sizes, d_1 and d_2, where d_1 is larger than d_2 [35]. The effect of decreasing the grain size for tensile testing is two-fold. First, the three flow regions of I, II and III are displaced to faster strain rates so that superplasticity is achieved more quickly. Second, larger elongations are attained at faster rates because less time is then available for the interlinkage of internal cavities that ultimately lead to failure.

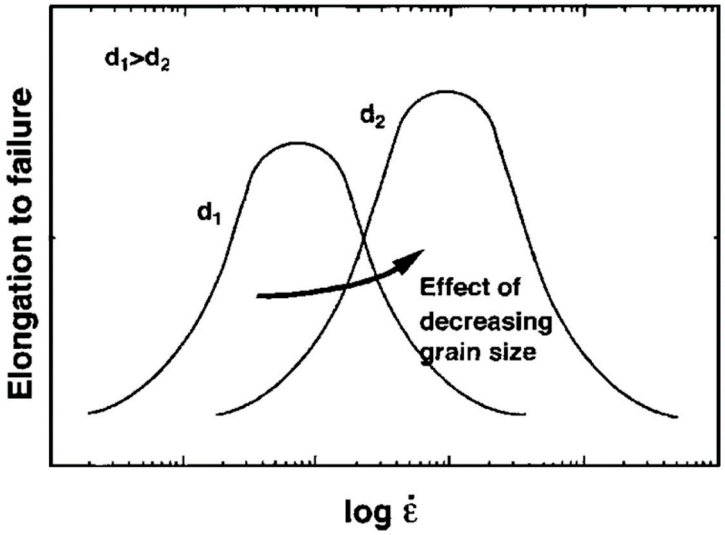

Figure 7. Schematic illustration of elongation to failure versus strain rate showing the effect of decreasing the grain size [35].

The first experimental demonstration of the potential for achieving high strain rate superplasticity after SPD processing was presented in 1997 using a commercial Al-5.5% Mg-2.2% Li-0.12% Zr alloy, as illustrated in Figure 8 [36]. This alloy was processed by ECAP to produce a grain size of ~1.2 μm and it was then pulled in tension at a temperature of 623 K using rapid strain rates of either 10^{-2} or 10^{-1} s^{-1}. In Figure 8, the upper sample is untested, the second sample was pulled at 10^{-2} s^{-1} and the test was discontinued without failure at an elongation of 1180% and the lower sample was pulled to failure at 10^{-1} s^{-1} to give a total elongation of 910%. These results provide excellent examples of high strain rate superplasticity and inspection of the sample tested at 10^{-2} s^{-1} in Figure 8 shows that the superplastic sample pulls out without any visible necking within the gauge length, where this uniform deformation is an important requirement for true superplasticity [37].

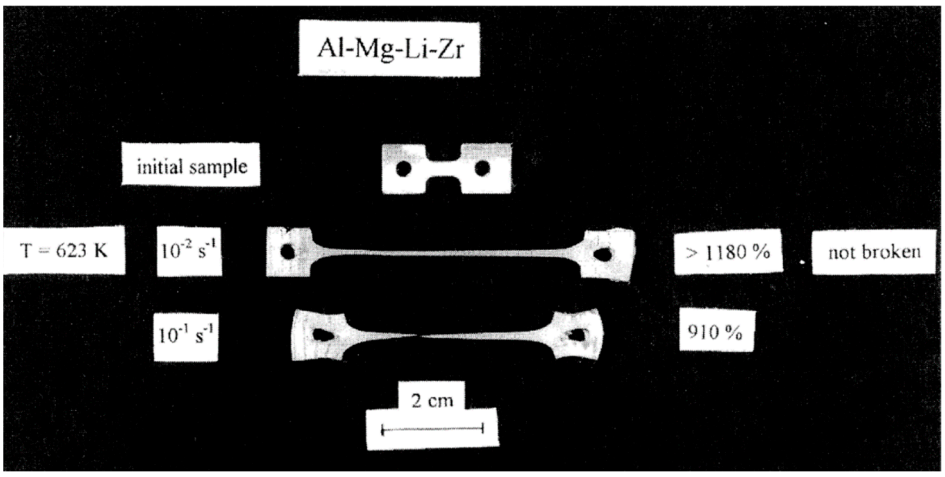

Figure 8. Examples of high strain rate superplasticity in an Al–Mg–Li–Zr alloy pulled at strain rates of 10^{-2} and 10^{-1} s^{-1} [36].

Although the laboratory data in Figure 8 provide a clear demonstration of the occurrence of high strain rate superplasticity, it is important to demonstrate that this effect can be easily utilized for the superplastic forming operations that are necessary to fabricate intricate curved parts for use in industrial applications. Accordingly, disks of an Al-3% Mg-0.2% Sc alloy having diameters of ~0.3 mm were cut perpendicular to the longitudinal

axes of billets processed by ECAP, and they were then inserted individually in a biaxial gas-pressure superplastic forming facility where they were clamped around the periphery and subjected on the lower surface to a constant pressure of an argon gas for very short periods of time. A gas pressure of 1.0 Mpa was used in these experiments to provide a direct comparison with the gas pressures generally employed in industrial superplastic forming operations. Figure 9 shows typical results where the disk at (a) was not subjected to any gas pressure and the disks at (b) and (c) were subjected to gas pressure for very short periods of 30 s and 60 s, respectively [38]. It is readily apparent that the disks at (b) and (c) have formed into domes and careful measurements on the dome processed for 60 s showed there was reasonably uniform thinning at all points on the surface. This result demonstrates that excellent superplastic forming capabilities may be achieved in these materials and the speed of processing is especially attractive because it avoids the relatively long forming times, typically of the order of ~20 min, which are a characteristic feature of many superplastic forming operations.

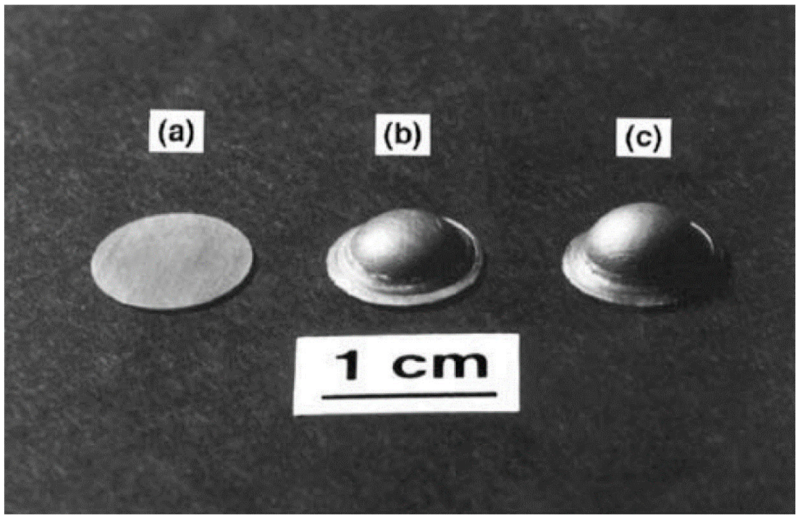

Figure 9. Examples of domes formed in an Al–Mg–Sc alloy after imposing a pressure of 1.0 MPa for (**a**) 0, (**b**) 30 and (**c**) 60 s, respectively [38].

5. The Development of Superplasticity using other SPD processing Procedures

The experimental results shown in Figures 6, 8 and 9 relate to samples prepared using the ECAP processing technique but other SPD techniques are also available and they provide an opportunity for achieving excellent superplastic elongations.

For example, in high-pressure torsion (HPT), the sample, usually in the form of a thin disk, is compressed between massive anvils and then subjected to torsional straining [39]. Processing by HPT has an advantage over ECAP because it produces materials with smaller grain sizes [40,41] and also it leads to a higher fraction of grain boundaries having high angles of misorientation [42], where this latter effect is important for achieving GBS during the flow process. A recent review summarized the development of superplasticity in materials processed by HPT [43] and there is also a comprehensive tabulation of superplasticity in Al–Mg–Sc alloys when processed by HPT and other procedures [44]. Figure 10 shows an example of an elongation of 1600% achieved in an HPT sample of an Al-3% Mg-0.2% Sc alloy processed by HPT for 2 revolutions at room temperature under an applied pressure of 1.0 GPa and then pulled to failure at 573 K using a strain rate of 3.3×10^{-3} s^{-1} [45].

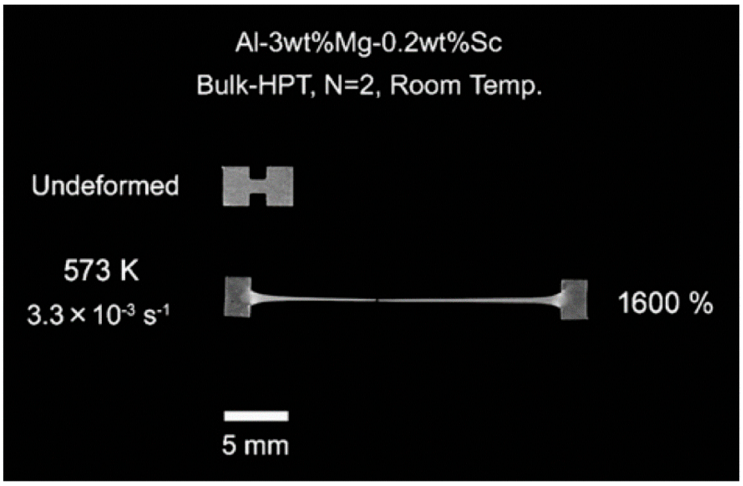

Figure 10. An example of superplasticity in an Al–Mg–Sc alloy processed by HPT [45].

Another important SPD procedure is tube high-pressure shearing (t-HPS), where a tubular sample is subjected to shearing under high hydrostatic pressure [46,47]. Experiments were conducted by subjecting two Pb-Sn alloys, Pb-40% Sn and Pb-62% Sn, to t-HPS and then pulling tensile samples to failure at a strain rate of 1.0×10^{-3} s^{-1}. The experimental results are shown in Figure 11, where the plots of engineering stress against engineering strain include the t-HPS samples plus samples of the same alloys prepared in the cast and rolled conditions [48]. It is readily apparent that the cast and rolled samples are not superplastic with elongations of <200%, but both alloys exhibit superplasticity after processing by t-HPS with a maximum elongation of ~1870% in the Pb-40% Sn alloy. It is important to note that the average grain size in this alloy was ~1.0 μm after the t-HPS processing, and the composition consisted of homogeneously mixed domains of Pb and Sn in almost equal proportions.

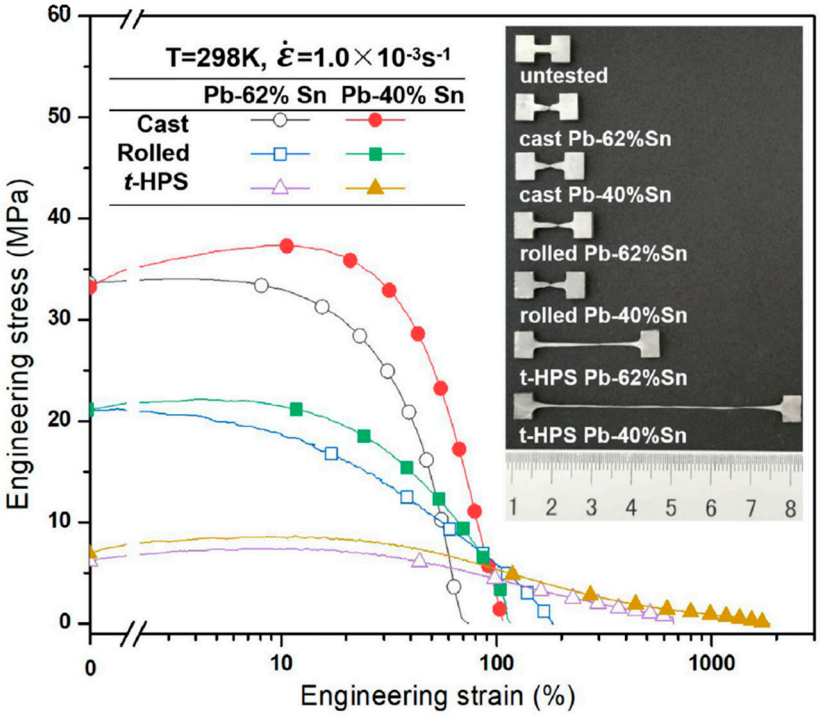

Figure 11. Examples of superplasticity in two Pb–Sn alloys processed by tube high-pressure shearing [48].

Finally, it is important to note that, in addition to achieving superplasticity at rapid strain rates in ultrafine-grained materials, it is also possible to achieve superplastic elongations at unusually low temperatures. This low temperature superplasticity was first reported almost twenty years ago in materials processed by ECAP, as, for example, in a tensile elongation of ~800% in an Mg-9% Al alloy at a temperature of 423 K [49] and an elongation of ~460% in an AZ31 Mg alloy also at 423 K [50]. More recently, there have been similar reports of exceptional low temperature superplatsicity after processing by HPT, as in an Al–Zn–Mg–Zr alloy with an elongation of >500% at 443 K [51]. In practice, however, the development of high strain rate superplasticity generally has more relevance than low temperature superplasticity to the development of an industrial superplastic forming capability.

6. The Development of the Superplastic Forming Industry

Superplastic forming provides the opportunity for fabricating complex curved shapes by taking advantage of the excellent flow properties when superplastic alloys are processed within the superplastic region II. An early review published in 2007 provided a very comprehensive summary of the industrial processing, which is now used to superplastically form many thousands of tons of metallic sheet metal [52]. More recent developments are described in several detailed publications [53–56].

An early approach in industrial forming was to make use of the so-called quick plastic forming (QPF) technology, which is based on a hot-blow forming process operating within the flow regime of dislocation glide where $n = 3$, so that this is not a true superplastic behavior [57]. This QPF approach was adopted in order to fabricate large numbers of aluminum panels for use in automotive applications, but most commercial superplastic forming operations were conducted within the true superplastic range where $n = 2$ and $m = 0.5$.

A major player in superplastic forming was the Superform Company, which was founded in England in 1974 and, subsequently, in 1986, was established as Superform USA with a large facility in Riverside, California. One of the authors of this review had the pleasure of receiving a special plaque from Superform USA on the occasion of a symposium marking his 65th birthday, which was organized as part of the TMS Spring Meeting in San Francisco, California, in February 2005. The plaque is shown in Figure 12 [58], and it has two photographs of a high-performance sports car whose bodywork was made by superplastic forming at Superform USA in California. The wording in the central panel reads as follows: "From Frome to LA and all around the world in 65 years. What a trip! Prof. Terence G. Langdon. A preeminent shining light helping to illuminate our future. Congratulations from all at Superform."

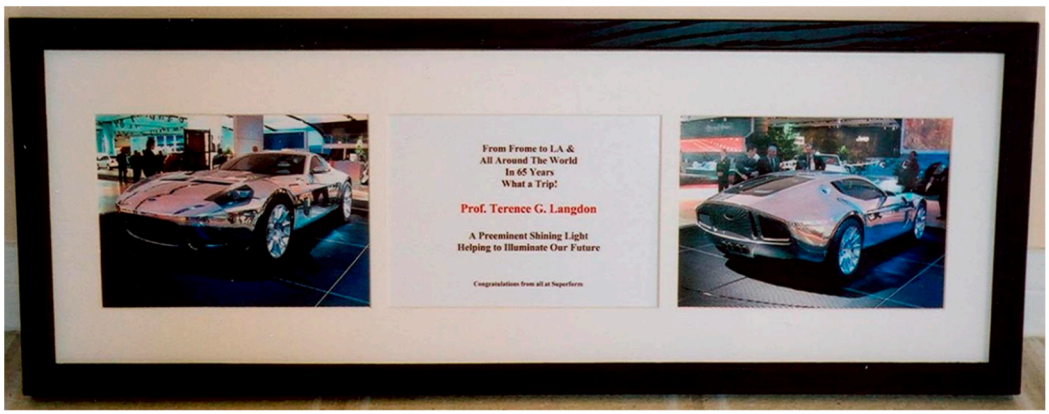

Figure 12. A plaque presented by Superform USA to one of the authors at a conference in San Francisco in 2005 [58].

7. Summary and Conclusions

1. Superplastic flow, in the form of an elongation of >1900%, was first reported in England in experiments conducted in 1934 but the result attracted little attention within the scientific community;
2. Later, following extensive superplastic research in the Soviet Union, research developed in western countries and this gradually built up an understanding of the flow process and the potential for optimizing the superplastic elongations;
3. Today, the superplastic forming industry plays a major role in the fabrication of complex parts for use in aerospace, automotive and many other applications, with the result that many tons of sheet metals are effectively processed every year.

Author Contributions: Conceptualization, J.W.-N. and T.G.L.; resources, J.W.-N. and T.G.L.; data curation, J.W.-N. and T.G.L.; writing—original draft preparation, J.W.-N. and T.G.L.; writing—review and editing, J.W.-N. and T.G.L.; visualization, J.W.-N. and T.G.L.; supervision, J.W.-N. and T.G.L.; project administration, J.W.-N. and T.G.L.; funding acquisition, T.G.L. All authors have read and agreed to the published version of the manuscript.

Funding: The work of one of us was supported by the European Research Council under ERC Grant Agreement No. 267464-SPDMETALS (T.G.L.).

Institutional Review Board Statement: Not applicable.

Informed Consent Statement: Not applicable.

Data Availability Statement: Not applicable.

Conflicts of Interest: The authors declare no conflict of interest.

References

1. Langdon, T.G. An analysis of flow mechanisms in high temperature creep and superplasticity. *Mater. Trans.* **2005**, *46*, 1951–1956. [CrossRef]
2. Langdon, T.G. Identifying creep mechanisms in plastic flow. *Z. Metallk.* **2005**, *96*, 522–531. [CrossRef]
3. Langdon, T.G. Grain boundary sliding revisited: Developments in sliding over four decades. *J. Mater. Sci.* **2006**, *41*, 597–609. [CrossRef]
4. Bengough, G.D. A study of the properties of alloys at high temperatures. *J. Inst. Metals* **1912**, *7*, 123–178.
5. Jenkins, C.H.M. Strength of Cd-Zn and Sn-Pb alloy solder. *J. Inst. Metals* **1928**, *40*, 21–32.
6. Pearson, C.E. The viscous properties of extruded eutectic alloys of lead-tin and bismuth-tin. *J. Inst. Metals* **1934**, *54*, 111–124.
7. Woodford, D.A. Strain-rate sensitivity as a measure of ductility. *Trans. ASM* **1969**, *62*, 291–293.
8. Mohamed, F.A.; Ahmed, M.M.I.; Langdon, T.G. Factors influencing ductility in the superplastic Zn-22 pct Al eutectoid. *Metall. Trans. A* **1977**, *8A*, 933–938. [CrossRef]
9. Ahmed, M.M.I.; Langdon, T.G. Exceptional ductility in the superplastic Pb-62 pct Sn eutectic. *Metall. Trans. A* **1977**, *8A*, 1832–1833. [CrossRef]
10. Nabarro, F.R.N. *Deformation of Crystals by the Motion of Single Ions*; Report of a Conference on Strength of Solids; The Physical Society: London, UK, 1984; pp. 75–90.
11. Herring, C. Diffusional viscosity of a polycrystalline solid. *J. Appl. Phys.* **1950**, *21*, 437–445. [CrossRef]
12. Coble, R.L. A model for boundary diffusion controlled creep in polycrystalline materials. *J. Appl. Phys.* **1963**, *34*, 1679–1682. [CrossRef]
13. Weertman, J. Creep of indium, lead and some of their alloys with various metals. *Trans AIME* **1960**, *218*, 207–218.
14. Weertman, J. Steady-state creep through dislocation climb. *J. Appl. Phys.* **1957**, *28*, 362–364. [CrossRef]
15. Bird, J.E.; Mukherjee, A.K.; Dorn, J.E. *Correlations between High-Temperature Creep Behavior and Structure. Quantitative Relation Between Properties and Microstructure*; Brandon, D.G., Rosen, A., Eds.; Israel Universities Press: Jerusalem, Israel, 1969; pp. 255–342.
16. Cottrell, A.H. *Report of a Conference on Strength of Solids*; The Physical Society: London, UK, 1948; pp. 30–38.
17. Weertman, J. Steady-state creep of crystals. *J. Appl. Phys.* **1957**, *28*, 1185–1189. [CrossRef]
18. Langdon, T.G. *Superplasticity: An Historical Perspective, Superplasticity in Advanced Materials*; Hori, S., Tokizane, M., Furushiro, N., Eds.; The Japan Society for Research on Superplasticity: Osaka, Japan, 1991; pp. 3–12.
19. Underwood, E.E. A review of superplasticity and related phenomena. *JOM* **1962**, *14*, 914–919. [CrossRef]
20. Backofen, W.A.; Turner, L.R.; Avery, D.H. Superplasticity in an Al-Zn alloy. *Trans. ASM* **1964**, *57*, 980–990.
21. Langdon, T.G. The mechanical properties of superplastic materials. *Metall. Trans. A* **1982**, *13A*, 689–701. [CrossRef]
22. Ishikawa, H.; Mohamed, F.A.; Langdon, T.G. The influence of strain rate on ductility in the superplastic Zn-22% Al eutectoid. *Phil. Mag.* **1975**, *32*, 1269–1271. [CrossRef]

23. Langdon, T.G. An evaluation of the strain contributed by grain boundary sliding in superplasticity. *Mater Sci. Eng. A* **1994**, *A174*, 225–230. [CrossRef]
24. Valiev, R.Z.; Langdon, T.G. An investigation of the role of intragranular dislocation strain in the superplastic Pb-62% Sn eutectic alloy. *Acta Metall. Mater.* **1993**, *41*, 949–954. [CrossRef]
25. Mohamed, F.A.; Langdon, T.G. Deformation mechanism maps for superplastic materials. *Scripta Metall.* **1976**, *10*, 759–762. [CrossRef]
26. Cannon, W.R.; Langdon, T.G. Review: Creep of ceramics, Part 2, An examination of flow mechanisms. *J. Mater. Sci.* **1988**, *23*, 1–20. [CrossRef]
27. Langdon, T.G. A unified approach to grain boundary sliding in creep and superplasticity. *Acta Metall. Mater.* **1994**, *42*, 2437–2443. [CrossRef]
28. Taleff, E.M.; Leseur, D.R.; Wadsworth, J. Enhanced ductility in coarse-grained Al-Mg alloys. *Metall. Mater. Trans. A* **1996**, *27A*, 343–352. [CrossRef]
29. Langdon, T.G. Seventy-five years of superplasticity: Historic developments and new opportunities. *J. Mater. Sci.* **2009**, *44*, 5998–6010. [CrossRef]
30. Valiev, R.Z.; Kaibyshev, O.A.; Kuznetsov, R.I.; Musalimov, R.S.; Tsenev, N.K. Low-temperature superplasticity of metallic materials. *Dokl. Akad. Nauk SSSR* **1998**, *301*, 864–866.
31. Valiev, R.Z.; Islamgaliev, R.K.; Alexandrov, I.V. Bulk nanostructured materials from severe plastic deformation. *Prog. Mater. Sci.* **2000**, *45*, 103–189. [CrossRef]
32. Valiev, R.Z.; Langdon, T.G. Principles of equal-channel angular pressing as processing tool for grain refinement. *Prog. Mater. Sci.* **2006**, *51*, 881–981. [CrossRef]
33. Komura, S.; Horita, Z.; Furukawa, M.; Nemoto, M.; Langdon, T.G. An evaluation of the flow behavior during high strain rate superplasticity in an Al-Mg-Sc alloy. *Metall. Mater. Trans. A* **2001**, *32A*, 707–716.
34. Higashi, K.; Mabuchi, M.; Langdon, T.G. High-strain-rate superplasticity in metalliv materials and the potential for ceramic materials. *ISIJ Intl.* **1996**, *36*, 1423–1438. [CrossRef]
35. Xu, C.; Furukawa, M.; Horita, Z.; Langdon, T.G. Achieving a superplastic forming capability through severe plastic deformation. *Adv. Eng. Mater.* **2003**, *5*, 359–364. [CrossRef]
36. Valiev, R.Z.; Salimonenko, D.A.; Tsenev, N.K.; Berbon, P.B.; Langdon, T.G. Observations of high strain rate superplasticity in commercial aluminum alloys with ultrafine grain sizes. *Scripta Mater.* **1997**, *37*, 1945–1950. [CrossRef]
37. Langdon, T.G. Fracture processes in superplastic flow. *Metal Sci.* **1982**, *16*, 175–183. [CrossRef]
38. Horita, Z.; Furukawa, M.; Nemoto, M.; Barnes, A.J.; Langdon, T.G. Superplastic forming at high strain rates after severe plastic deformation. *Acta Mater.* **2000**, *48*, 3633–3640. [CrossRef]
39. Zhilyaev, A.P.; Langdon, T.G. Using high-pressure torsion for metal processing: Fundamentals and applications. *Prog. Mater. Sci.* **2008**, *53*, 893–979. [CrossRef]
40. Zhilyaev, A.P.; Kim, B.K.; Nurislamova, G.V.; Baró, M.D.; Szpunar, J.A.; Langdon, T.G. Orientation imaging microscopy of ultrafine-grained nickel. *Scripta Mater.* **2002**, *46*, 575–580. [CrossRef]
41. Zhilyaev, A.P.; Nurislamova, G.V.; Kim, B.K.; Baró, M.D.; Szpunar, J.A.; Langdon, T.G. Experimental parameters influencing grain refinement and microstructural evolution during high-pressure torsion. *Acta Mater.* **2003**, *51*, 753–765. [CrossRef]
42. Wongsa-Ngam, J.; Kawasaki, M.; Langdon, T.G. A comparison of microstructures and mechanical properties in a Cu-Zr alloy processed using different SPD techniques. *J. Mater. Sci.* **2013**, *48*, 4653–4660. [CrossRef]
43. Kawasaki, M.; Langdon, T.G. Review: Achieving superplasticity in metals processed by high-pressure torsion. *J. Mater. Sci.* **2014**, *49*, 6487–6496. [CrossRef]
44. Pereira, P.H.R.; Huang, Y.; Kawasaki, M.; Langdon, T.G. An examination of the superplastic characteristics of Al-Mg-Sc alloys after processing. *J. Mater. Res.* **2017**, *32*, 4541–4553. [CrossRef]
45. Horita, Z.; Langdon, T.G. Achieving exceptional superplasticity in a bulk aluminum alloy processed by high-pressure torsion. *Scripta Mater.* **2008**, *58*, 1029–1032. [CrossRef]
46. Wang, J.T.; Li, Z.; Wang, J.; Langdon, T.G. Principles of severe plastic deformation using tube high -pressure shearing. *Scripta Mater.* **2012**, *67*, 810–813. [CrossRef]
47. Li, Z.; Zhang, P.F.; Yuan, H.; Lin, K.; Liu, Y.; Lin, D.L.; Wang, J.T.; Langdon, T.G. Principle of one-step synthesis for multilayered structures using tube high-pressure shearing. *Mater. Sci. Eng. A* **2016**, *658*, 367–375. [CrossRef]
48. Lin, K.; Li, Z.; Liu, Y.; Ma, E.; Wang, J.T.; Langdon, T.G. Exploiting tube high-pressure shearing to prepare a microstructure in Pb-Sn alloys for unprecedented superplasticity. *Scripta Mater.* **2022**, *209*, 114390. [CrossRef]
49. Matsubara, K.; Miyahara, Y.; Makii, K.; Horita, Z.; Langdon, T.G. Using extrusion and ECAP processing to achieve low temperature and high strain rate superplasticity. *Mater. Sci. Forum* **2003**, *419–422*, 497–502. [CrossRef]
50. Lin, H.K.; Huang, J.C.; Langdon, T.G. Relationship between texture and low temperature superplasticity in an extruded AZ31 Mg alloy processed by ECAP. *Mater. Sci. Eng. A* **2005**, *402*, 250–257. [CrossRef]
51. Chinh, N.Q.; Murashkin, M.Y.; Bobruk, E.V.; Lábár, J.L.; Gubicza, J.; Kovács, Z.; Ahmed, A.Q.; Maier-Kiener, V.; Valiev, R.Z. Ultralow-temperature superplasticity and its novel mechanism in ultrafine-grained Al alloys. *Mater. Res. Lett.* **2021**, *9*, 475–482.
52. Barnes, A.J. Superplastic forming 40 years and still growing. *J. Mater. Eng. Perform.* **2007**, *16*, 440–454. [CrossRef]

53. Mosleh, A.O.; Mikhaylovskaya, A.V.; Kotov, A.D.; Kwame, J.S. Experimental, modelling and simulation of an approach for optimizing the superplastic forming of Ti-6%Al-4%V titanium alloy. *J. Manufact. Proc.* **2019**, *45*, 262–272. [CrossRef]
54. Yasmeen, T.; Shao, Z.; Zhao, L.; Gao, P.; Lin, J.; Jiang, J. Constitutive modelling for the simulation of the superplastic forming of TA15 titanium alloy. *Intl. J. Mech. Sci.* **2019**, *164*, 105178. [CrossRef]
55. Yasmeen, T.; Zhao, B.; Zheng, J.H.; Tian, F.; Lin, J.; Jiang, J. The study of flow behavior and governing mechanisms of a titanium alloy during superplastic forming. *Mater. Sci. Eng. A* **2020**, *788*, 139482. [CrossRef]
56. Du, Z.; Zhang, K. The superplastic forming/diffusion bonding and mechanical property of TA15 alloy for four-layer hollow structure with squad grid. *Intl. J. Mater. Form.* **2021**, *14*, 1057–1066. [CrossRef]
57. Krajewski, P.E.; Schroth, J.G. Overview of quick plastic forming technology. *Mater. Sci. Forum* **2007**, *551–552*, 3–12. [CrossRef]
58. Langdon, T.G. The background to superplastic forming and opportunities arising from new developments. *Solid State Phenom.* **2020**, *306*, 1–8. [CrossRef]